DOI: 10.1002/cphc.201100669

# Long-Range Transport of Giant Vesicles along Microtubule Networks

Christoph Herold,[a] Cécile Leduc,[c, d] Robert Stock,[a] Stefan Diez,*[b, c] and Petra Schwille*[a]

We report on a minimal system to mimic intracellular transport of membrane-bounded, vesicular cargo. In a cell-free assay, purified kinesin-1 motor proteins were directly anchored to the membrane of giant unilamellar vesicles, and their movement studied along two-dimensional microtubule networks. Motion-tracking of vesicles with diameters of 1–3 μm revealed traveling distances up to the millimeter range. The transport velocities were identical to velocities of cargo-free motors. Using total internal reflection fluorescence (TIRF) microscopy, we were able to estimate the number of GFP-labeled motors involved in the transport of a single vesicle. We found that the vesicles were transported by the cooperative activity of typically 5–10 motor molecules. The presented assay is expected to open up further applications in the field of synthetic biology, aiming at the in vitro reconstitution of sub-cellular multi-motor transport systems. It may also find applications in bionanotechnology, where the controlled long-range transport of artificial cargo is a promising means to advance current lab-on-a-chip systems.

## 1. Introduction

Cytoskeletal motor proteins are essential for organizing the intracellular space, including the transport of cargos such as small vesicles and entire cell organelles. Among these motors, kinesin-1 is one of the best understood, due to intense research over the past two decades. It moves processively towards the plus end of a microtubule, converting the chemical energy released by adenosine triphosphate (ATP) hydrolysis into mechanical work. It was used for in vitro studies to move microtubules in a gliding assay over a surface of immobilized motors,[1] or in the inverted situation, to transport beads along immobilized microtubules.[2] Single-molecule experiments revealed, among other properties, a step size of 8 nm[3] and a processivity of approximately 800 to 1200 nm.[4,5] Since the number of motor proteins transporting cargos in vivo is thought to be larger than one,[6] in recent years the focus shifted towards studying the cooperativity of multiple motors. With several processive motor proteins working together, large transport distances for cargos such as beads could be reached.[7,8,9] Thereby, the traveling velocity does not change if several kinesin molecules are transporting a cargo with a negligible drag force,[1,7,9] compared to the approximately 6 pN stall force of a single kinesin-1 motor.[10] Additionally, multiple motors which cooperatively act together can develop large forces, an effect used to pull membrane tubes from giant liposomes.[11,12]

To mimic the in vivo situation of transport by motor proteins, which are diffusively attached to membranous cargo, systems with motors anchored to the lipids of fluid membranes are desirable. Although endosomes from cytosolic extracts would feature such motor mobility on the cargo, the disadvantage of extract-based assays is the relatively low control over the single components. For example, different types of motors such as kinesin and dynein might be attached to the same endosome.[13,14] These ambiguities can be overcome by setting up a controllable assay using artificial vesicles of defined lipid composition, purified motors and known buffer ingredients. Besides resembling in vivo transport processes, the use of such assays based on fluid cargos is of interest in lab-on-chip delivery systems for the controlled distribution of specific amounts of material, as recently demonstrated in an assay of kinesin-transported oil droplets.[15]

Herein, we report on the transport of artificial giant unilamellar vesicles by multiple kinesin-1 motor proteins directly anchored to the fluid membrane. We determined the transport velocity of the vesicles and found it to be in accordance with the velocity of cargo-free single kinesin-1 molecules. Traveling distances of the order of one millimeter were reached. Deviations from transport at maximum velocity were only observed

[a] C. Herold, R. Stock, Prof. Dr. P. Schwille
Biophysics, BIOTEC, Technische Universität Dresden
Tatzberg 47/49, 01307 Dresden (Germany)
Fax: (+49) 351-46340342
E-mail: schwille@biotec.tu-dresden.de

[b] Prof. Dr. S. Diez
B CUBE—Center for Molecular Bioengineering
Technische Universität Dresden
Arnoldstr. 18, 01307 Dresden (Germany)
E-mail: diez@bcube-dresden.de

[c] Dr. C. Leduc, Prof. Dr. S. Diez
Max Planck Institute of Molecular Cell Biology and Genetics
Pfotenhauerstraße 108, 01307 Dresden (Germany)

[d] Dr. C. Leduc
Laboratoire Photonique, Numérique et Nanosciences
IOGS, Université de Bordeaux, CNRS
351 cours de la libération, 33405 Talence (France)

Supporting information for this article is available on the WWW under http://dx.doi.org/10.1002/cphc.201100669.

 © 2012 Wiley-VCH Verlag GmbH & Co. KGaA, Weinheim 

when the vesicles simultaneously interacted with non-parallel microtubules.

## 2. Results and Discussion

His-tagged kinesin-1 motors were attached to vesicles (giant liposomes or giant unilamellar vesicles) either via streptavidin linking biotinylated antibodies against the C-terminal His-tag of the motor proteins to biotinylated anchor lipids, or via direct interaction of kinesin's His-tag to nickel-chelating anchor lipids (Figure 1a and Experimental Section). After the motor–

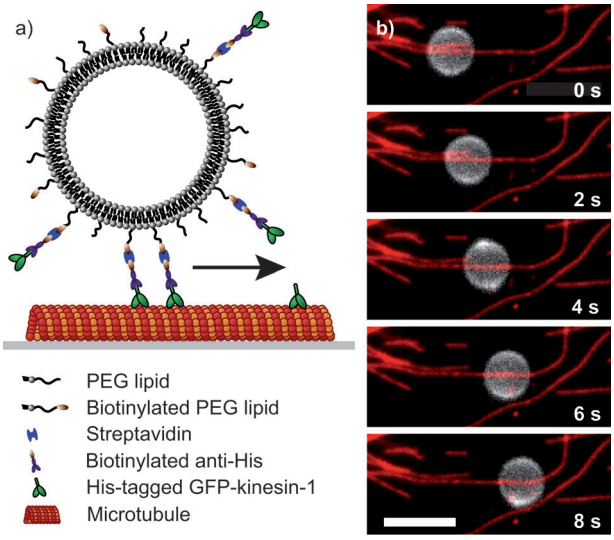


**Figure 1.** Unidirectional vesicle transport along microtubules. a) Schematic diagram of the transport experiment. His-tagged GFP-kinesin-1 motors were linked to the lipid membrane via biotinylated anti-His antibodies, streptavidin molecules and biotinylated PEG anchor lipids (not drawn to scale). Alternatively, the His-tagged kinesin-1 was directly bound to nickel-chelating anchor lipids in the membrane (not shown). b) Dual-colour, time-lapse micrographs of a typical transport event. Images of the equatorial plane of a vesicle (gray) are overlaid to an image of surface-immobilized microtubules (red). Scale bar 5 μm.

vesicle complexes had formed on the surface-immobilized microtubules, the transport process started and could be followed by observing the vesicle center moving unidirectionally along the microtubules (see Figure 1b and Supporting Information, Movie 1, for typical examples). To enable vesicle transport without strong deformation of the membrane, as formerly observed in membrane tube pulling assays,[11,12] a high membrane tension outside the tube pulling regime[12] was ensured by a higher osmolarity of the solution inside the vesicles compared to the surrounding motility buffer.

### 2.1. Traveling Distance of Transported Vesicles

Once a vesicle had attached to the microtubule network, various transport scenarios evolved: i) Vesicles were unidirectionally transported to the end of one microtubule and stayed there for the remaining time of observation; ii) vesicles started to move along one microtubule, but continued their travels on a neighboring microtubule. In the latter, the force of the motors attached to the new microtubule was presumably large enough to facilitate switching.[16] For both cases, we note that transport of vesicles with diameters larger than 1 μm always occurred over distances significantly longer than the processivity of individual kinesin-1 motors (about 1 μm), and detachment from the microtubules was never observed. These findings can be explained by the simultaneous action of multiple motors, where fast rebinding of previously detached motors prevents microtubule–vesicle separation.[7,8] In our experiments, the concentrations of anchor lipids and kinesin-1 motors were purposefully chosen such that capitalization on this effect was ensured. Sometimes, the geometry of the microtubule network led to vesicle movement in closed loops (Supporting Information, Movies 2 and 3), allowing for ultralong travelling distances, as shown in Movie 3 of the Supporting Information, that displays 20 out of 28 recorded rounds of vesicle transport in a 22.5 μm loop, resulting in a total of 0.63 mm.

### 2.2. Kinesin Patterns and Number of Transporting Motors

An estimate on the total number of GFP-kinesin-1 motors actively participating in single-vesicle transport can be derived from the GFP fluorescence recorded by total internal reflection fluorescence (TIRF) microscopy. Because the evanescent field only excites GFP-labeled motors close to the coverslip surface, the recorded GFP images exclusively depict the transporting motors on the bottom of the vesicles (Figure 2a). Most commonly, we observed a point-like kinesin pattern (Figure 2a, i) at the lower pole of the vesicle. Interestingly, we frequently also found other shapes, like stretched spots (Figure 2a, ii), rings (Figure 2a, iii) and double points (Figure 2a, iv). We attribute this variety of kinesin patterns to the fact that the DOPC vesicle membrane does not represent a hard shell, but rather constitutes a fluid system being deformable by the motor forces. Note that all kinesin patterns shown in Figure 2a were recorded from the same vesicle, that is, they transformed into each other as the vesicle was transported along the microtubules (see also Movie 4 of the Supporting Information).

To estimate the number of GFP-kinesin-1 motors in close proximity to the microtubules, events of stable point-like kinesin patterns during vesicle transport were analyzed. In particular, we fitted the GFP signal (after background-subtraction) to a two-dimensional Gaussian and divided the resulting spot intensity by the average fluorescence intensity of a single GFP-kinesin-1 motor not anchored to any vesicle. The resulting normalized intensity suggests that the number of motors capable of participating in vesicle transport fluctuated strongly between values of 2 and 20 (Figure 2b). These fluctuations can again be attributed to the fluid state of the DOPC membrane, allowing rapid diffusion of the anchor lipids and bound GFP-kinesin-1 motors not interacting with the microtubules [diffusion coefficient $D = 6.0 \pm 1.1\ \mu m^2 s^{-1}$ (mean $\pm$sd, $N = 14$) measured by scanning fluorescence correlation spectroscopy, FCS].

Note that in our experiments the number of kinesin-1 molecules in the flow chamber was determined by the density of the microtubule network to which the motors were initially

 © 2012 Wiley-VCH Verlag GmbH & Co. KGaA, Weinheim 

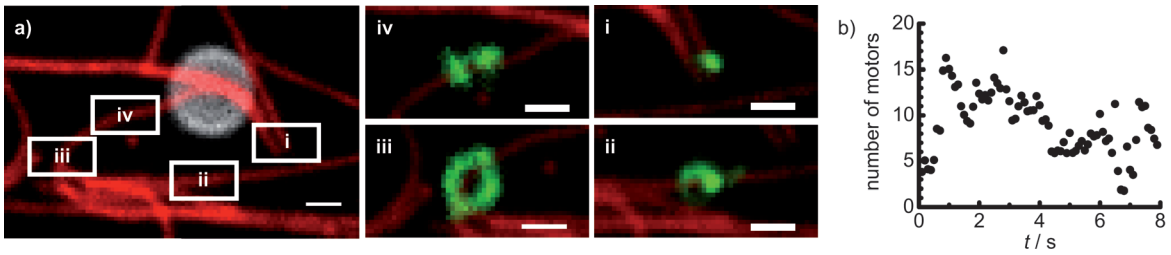


**Figure 2.** Dynamic distribution of GFP-kinesin-1 motors during vesicle transport. a) Color-combined fluorescent micrographs of GFP-kinesin-1 molecules recorded using TIRF microscopy (green) in the microtubule–vesicle interaction plane, that is, on the bottom of a transported vesicle (gray, equatorial plane) and on top of the surface immobilized microtubule network (red). Scale bars 1 μm. Different patterns of the motor proteins (recorded at different positions i–iv) transformed into each other during transport. i) Point-like kinesin pattern as expected on the bottom of a spherical vesicle. Other kinesin patterns, such as ii) a stretched spot, iii) a ring and iv) a double point, are only possible due to the deformation of the fluid vesicle membrane. b) Normalizing the intensities recovered from tracking GFP-kinesin-1 molecules (arranged in a point-like accumulation on the bottom of a transported vesicle) to the intensities of single (cargo-free) GFP-kinesin-1 motors allows an estimation of the number of motors involved in transport.

bound to in the presence of AMP-PNP. We found that the number of kinesin-1 motors involved in the vesicle transport did not change if the number of biotinylated lipids was reduced from 1 mol% to 0.1 mol%. For further reduction to 0.01 mol% of biotinylated lipid anchors, transport events became rare and no long-range transport was observed. We estimate that on a spherical vesicle with 2 μm diameter and an area per lipid of 0.72 $nm^2$,[17] approximately 1.3 (for 0.01 mol% anchor lipids to total lipids) and 13 (for 0.1 mol% anchor lipids to total lipids) anchor lipids were within 4 to 16 nm distance to a microtubule, allowing membrane bound kinesin-1 motors to interact with a microtubule[7] (for details see Figure S1 of the Supporting Information). This estimate is based on the assumption of a homogeneous distribution of the anchor lipids before the initial vesicle–microtubule interaction. Once contact between a vesicle and the microtubule was established, membrane-anchored kinesin-1 molecules possibly were recruited at the microtubule. Our observations indicate that 1.3 kinesin-1 molecules were not sufficient to initiate or maintain the interaction between diffusing vesicles and the rather sparse microtubule network. Using NTA-His binding demanded for higher concentrations of the anchor lipids (5 mol%), since already at 2 mol% transport events were significantly reduced, an effect most probably caused by a lower binding affinity of the NTA-His compared to the streptavidin–biotin interaction.

### 2.3. Transport Stalling and Bidirectional Motion

Occasionally, the vesicles stalled during their movement along the microtubule networks. These events most likely resulted from scenarios where the vesicle-bound motors simultaneously interacted with nearby microtubules of different orientation. Especially, large vesicles (diameter $>$ 5 μm) were often affected by this phenomenon. We believe that the smaller curvature of the larger vesicles allowed motor–microtubule interactions over a larger area of the microtubule network. As a consequence, we found the optimal vesicle diameter for long-range transport to be between 1 and 3 μm. This size allowed the vesicles to switch between microtubules for continuous transport (bridging gaps of up to 0.5 μm) but rarely caused long-term stalling at microtubule intersections.

If vesicles interacted with anti-parallel microtubules, bidirectional motion was observed from time to time (Figure 3). The kinesin-1 molecules on the different microtubules then engaged in a tug-of-war, trying to pull the vesicle in opposite directions. Depending on which group of motors developed the stronger force, the vesicle either stalled, rapidly switched direction, or continued their movement in one direction[18] (see also Movie 5 of the Supporting Information).

### 2.4. Transport Velocities

The velocity of the transported vesicles was determined along straight and isolated microtubules, where the movement was

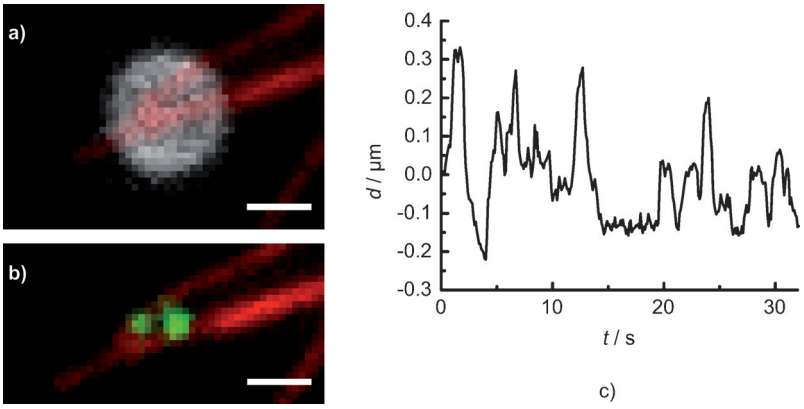


**Figure 3.** Stalling and bidirectional movement. a) Dual-color micrograph of the equatorial plane of a vesicle (gray) sitting on two anti-parallel microtubules (red). b) GFP-kinesin-1 molecules (green) observed by TIRF microscopy at the bottom of the vesicle attached to the different microtubules (red). Scale bar 1 μm. c) The travelled distance *d* of the center of mass of the vesicle is displayed over time *t*. A constant position *d* as visible between $t = 14$ s and $t = 18$ s indicates complete stall of the vesicle. Repeated changes in the traveling direction were observed.

 © 2012 Wiley-VCH Verlag GmbH & Co. KGaA, Weinheim 

not affected by motor interactions with nearby microtubules. All experiments were carried out under saturated ATP (1 mM) conditions to allow the GFP-kinesin-1 motors to travel at their maximum velocity. Under these conditions, vesicles (diameter of 1 to 3 μm) were found to move at $0.71 \pm 0.08\ \mu m\,s^{-1}$ (mean ± standard deviation (sd), $N = 68$, see Figure 4). This observation compared very well to single motors (not anchored to the membrane) which moved with a velocity of $0.72 \pm 0.12\ \mu m\,s^{-1}$ (mean ± sd, $N = 82$, see Figure S2 of the Supporting Information). Such agreement was not unexpected. Using Stokes law to calculate the viscous drag force $F = 6\pi\eta r v$ of a vesicle with hydrodynamic radius $r = 5\ \mu m$ transported at $v = 1\ \mu m\,s^{-1}$ in water of viscosity $\eta = 1$ mPa s, yields $F = 0.05$ pN. This force is two orders of magnitude smaller than the approximately 6 pN stall force of a single kinesin-1 motor,[10] and should not impact transport. However, we note that the addition of polyethylene glycol lipids (5 mol%) to the membrane was necessary to reduce unspecific interactions between the vesicles and the glass surface. If this precaution was not met, transport was often non-continuous, and transport velocities did not exceed $0.3\ \mu m\,s^{-1}$.

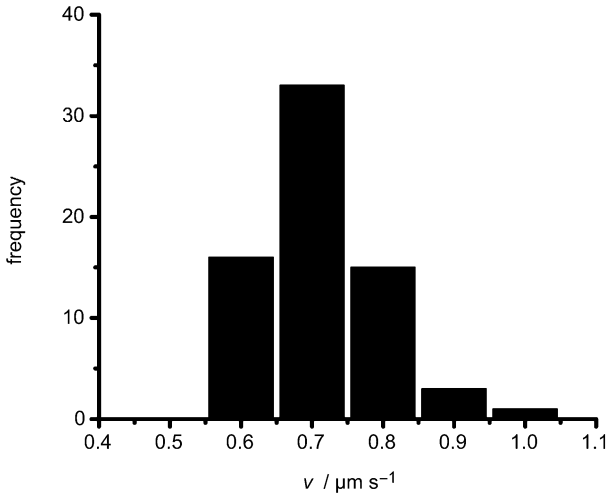


**Figure 4.** Histogram of the vesicle-transport velocities *v*. The velocities were measured when vesicles were transported along straight and isolated microtubules. The average vesicle-transport velocity was $0.71 \pm 0.08\ \mu m\,s^{-1}$.

### 2.5. Comparison of Different Strategies in Motor–Vesicle Coupling

The two different methods deployed to anchor GFP-kinesin-1 to vesicles either using biotinylated or NTA lipids led to an identical phenomenology of long-range transport, including switching between microtubules and traveling with velocities similar to single, cargo-free kinesin-1 molecules. Because the approach of directly anchoring GFP-kinesin-1 to the DGS-NTA lipids in the vesicle membrane involves fewer experimental steps compared to linking kinesin-1 to biotinylated lipids via streptavidin and biotinylated anti-His antibodies, this strategy may be favored in future applications. Additionally, working without streptavidin eliminates problems arising from possible cross-linking of the biotinylated vesicles, due to trace amounts of free streptavidin.

## 3. Conclusions

We established a reliable cell-free transport assay for giant vesicles, with diameters between 1 and 3 μm, carried along microtubule networks by multiple GFP-kinesin-1 motors. Such a transport system mimics the in vivo situation much closer than bead assays, since it allows for motion and diffusion of the anchored motor on the cargo's soft and fluid shell. As a result, the motor concentration at the transport site does not remain constant, but fluctuates, as shown by fluorescence intensity measurements of GFP-kinesin-1 molecules at the bottom of the vesicle in contact with the microtubule network. Generally, more than one (sometimes up to 20) motors were involved in vesicle transport. However, the velocity of the transported vesicles matched the velocity of single cargo-free kinesin-1 molecules in the same samples, in agreement with previously published results for beads[7] or oil droplets[15] that showed a constant velocity regardless of the number of motors transporting the cargo. Those results make us confident that unspecific interactions of the vesicles with the glass surface are negligible due to the use of 5 mol% PEGylated lipids. Reduced velocities, bidirectional movement or even complete stalling of the transport at times can be explained by the interaction of the vesicle-anchored kinesins with microtubules non-parallel to each other. Therefore, the proposed vesicle-transport assay can be employed to further understand interactions (including tug-of-war scenarios) of different motor proteins diffusively anchored to their cargo. Furthermore, the long vesicle traveling distances in the millimeter range, in case the arrangement of the microtubule network allowed for it, are of great interest for use in synthetic on-chip devices.[19] Those applications usually demand active, long-distance transport and/or sorting of controlled amounts of material that could be encapsulated inside the vesicle or attached to its membrane.

## Experimental Section

### Materials

DOPC (1,2-dioleoyl-sn-glycero-3-phosphocholine), mPEG-DOPE (1,2-dioleoyl-sn-glycero-3-phosphoethanolamine-*N*-[methoxy(polyethylene glycol)-2000]), DSPE-PEG-biotin (1,2-distearoyl-sn-glycero-3-phosphoethanolamine-*N*-[biotinyl(polyethylene glycol)2000]), DGS-NTA (1,2-dioleoyl-sn-glycero-3-[(*N*-(5-amino-1-carboxypentyl)iminodiacetic acid)succinyl]), were purchased from Avanti Polar Lipids (AL, USA). The lipid analogue dye DiD (1,1′-dioctadecyl-3,3,3′,3′-tetramethylindodicarbocyanine), fluorescein-labeled streptavidin and Pluronic F127 were bought from Invitrogen (CA, USA). The experiments were conducted in BRB80 as the working buffer, consisting of 80 mM PIPES [Piperazine-1,4-bis(2-ethanesulfonic acid)), 1 mM MgCl2, 1 mM EGTA (ethylene glycol-bis(2-aminoethylether)-tetraacetic acid) and KOH to regulate pH to 6.85. All chemicals as well as catalase, glucose oxidase, glucose, DTT (dithiothreitol), paclitaxel, DMSO (dimethylsulfoxid) and anti-β-tubulin were purchased from Sigma–Aldrich (MO, USA). Bovine brain tubulin and fluores-

 © 2012 Wiley-VCH Verlag GmbH & Co. KGaA, Weinheim 

cently labeled rhodamine-tubulin were bought from Cytoskeleton (CO, USA), penta-His-biotin antibody was obtained from Qiagen (Germany), GTP (guanosine-5′-triphosphate), ATP (adenosine-5′-triphosphate) and AMP-PNP (5′-adenylyl-β,γ-imidodiphosphate) were purchased from Roche (Germany) and streptavidin was bought from Thermo Scientific (Germany). GFP labeled truncated kinesin-1 with a C-terminal His-tag (rkin430-GFP) was used in all experiments.[20]

### Vesicle Formation

Vesicles were grown in 500 mOsm $kg^{-1}$ sucrose/glucose (50/50 molar ratio) solution using the standard electroformation method.[21] In brief, 2 μL of the lipid mixture (10 mg $mL^{-1}$ in chloroform) were spread and dried on two indium tin oxide (ITO) coated glass slides. The formation chamber was assembled using the ITO electrodes facing each other, spaced and sealed by a rubber ring (diameter 11 mm, height 3 mm). Approximately 300 μL of the glucose/sucrose solution was filled into the chamber and a sinusoidal ac field of 10 Hz and 1.4 V (rms) was applied for 30 min to obtain a large fraction of vesicles with a diameter of 1–3 μm. Two different types of vesicles with different membrane anchors were produced. For the nickel-chelating anchor, the lipid mixture contained 90 mol% DOPC, 5 mol% mPEG-DOPE and 5 mol% DGS-NTA, for the biotin anchor the mixture consisted of 95 mol% DOPC, 4 mol% mPEG-DOPE and 1 mol% DSPE-PEG-biotin. Additionally, 0.5 mol% DiD was added to visualize the membrane in fluorescence imaging microscopy.

### Microtubules

Microtubules were polymerized from a 1:3 mixture of rhodamine-labeled and unlabeled tubulin (32 μM) in BRB80 buffer additionally containing GTP (4 mM), MgCl2 (16 mM) and DMSO (2.7 M). This mixture was incubated at 37 °C for about an hour yielding microtubules of up to 100 μm in length. At the end of the incubation time, paclitaxel (10 μM) was added to stop the polymerization process and stabilize the microtubules. The microtubule solution was diluted 100-fold and centrifuged to remove non-polymerized tubulin.

### Oxygen Scavenger Solution

To reduce photobleaching of the fluorescent dyes, an oxygen scavenger system containing catalase (3 μM), glucose oxidase (12.5 μM), glucose (20 μM) and DTT (10 μM) in BRB80 was used.

### Vesicle Transport Assay

The general outline of the stepping assay and the flow chamber design were adapted from previously published works[12,22] and altered for optimal vesicle-transport results. Vesicle-transport experiments were carried out in flow chambers (typically 18 mm in length, 3 mm in width and 0.15 mm in height) constructed from two silanized glass cover slips separated by parafilm strips. Chemicals were consecutively flowed into the chamber in volumes of 20 μL and incubated at room temperature. The assay was conducted as follows: i) The anti-β-tubulin antibody (20 μg $mL^{-1}$ in BRB80) was injected into the chamber and incubated for 5 min. ii) The hydrophobic glass surface not covered with antibody was passivated by incubation with F127 (100 mg $mL^{-1}$ in BRB 80) for about 20 min.[23] iii) The chamber was rinsed with BRB80 and microtubules were inserted and incubated for about 10 min. iv) The chamber was rinsed again and afterwards incubated with casein (10 mg $mL^{-1}$ in BRB80) and additional paclitaxel (10 μM). v) A mixture of GFP-kinesin-1 molecules (10 nM) and AMP-PNP (10 μM) was injected. Incubation for 5 min allowed the kinesin molecules to bind to the microtubules, where they remained stationary due to the non-hydrolysable AMP-PNP. vi) Unbound kinesin-1 was washed out with buffer containing the oxygen scavenger system and in the last step, vesicles were bound to GFP-kinesin-1 employing two different techniques depending on the membrane anchor system: a) Streptavidin—biotin system: biotinylated penta-His-antibody (4 μg $mL^{-1}$) in BRB80 was added and incubated for 5 min to bind to the C-terminal His-tag of the kinesin-1 motors. After washing, streptavidin (0.5 mg $mL^{-1}$) with AMP-PNP (10 μM) was added and incubated for another 5 min, allowing the binding of streptavidin to the biotin sequence of the penta-His-antibody bound to the kinesin-1. After another washing step, the motility buffer was added. It consisted of BRB80 with paclitaxel (10 μM), ATP (1 mM), casein (200 μg $mL^{-1}$) and 8 vol% oxygen scavenger solution as well as 10 vol% of glucose/sucrose solution containing vesicles with the DSPE–PEG–biotin anchor. Thus, complexes of GFP-kinesin-1 with vesicle cargo attached via streptavidin-biotin were formed. b) DGS–NTA system: no intermediate steps were necessary. After binding of GFP-kinesin-1 to the microtubules, the motility buffer with 10 vol% of the DGS-NTA vesicle solution was added. The anchor lipids directly bound to the C-terminal His-tag of the kinesin-1. A single chamber was sealed and used for measurements up to two hours, during this time no signs of sample deterioration were noticed, suggesting that ATP depletion during this time span was of no concern.

To control the membrane tension of the vesicles, the osmolarity of the motility buffer was set to about 480 mOsm $kg^{-1}$, being 20 mOsm $kg^{-1}$ lower than the glucose/sucrose solution inside the vesicles. The osmolarity was measured using a micro osmometer (Model 210, Fiske Associates, MA, USA) and adjusted by adding small amounts ($<1$%) of DMSO to the motility buffer, since it facilitated a strong increase in the osmolarity of the buffer solution (about 150 mOsm $kg^{-1}$ per 1% DMSO). The total concentration of DMSO in the motility buffer, originating from the stock solution of the paclitaxel and the adjustment of the osmolarity, was about 1.5%. Since DMSO might be able to pass the vesicle membrane, the 20 mOsm $kg^{-1}$ osmolarity difference between the solutions inside and outside the vesicles constituted a lower limit. We found that under the conditions described above, the osmotic pressure and therefore the membrane tension, efficiently inhibited membrane tube pulling. Moreover, the density difference between the motility buffer and the glucose/sucrose solution inside the vesicles facilitated sedimentation of vesicles onto the microtubule network.

### Fluorescence Microscopy

Epifluorescence wide-field microscopy with fluorescence excitation through an HBO lamp (high-intensity short arc mercury lamp) and appropriate filter cubes was used to image the rhodamine labeled microtubule network and transported vesicles containing the DiD membrane label. Total internal reflection fluorescence (TIRF) microscopy, based on excitation with the 488 nm line of an argon laser and appropriate filters, was used to image the GFP-kinesin-1 molecules. Fluorescence microscopy imaging was carried out using either a Leica AF6000 LX TIRF system with an HCX PLAN APO 100x oil immersion objective, numerical aperture (NA) 1.46, or a Zeiss Axiovert 200 M inverted microscope fitted with a Zeiss TIRF system and a Zeiss C-Apochromat 100x oil immersion objective, NA 1.46. On both setups, the fluorescence signal was detected via an Andor iXon 897 EM-CCD camera. The exposure time was set to 100 ms.

 © 2012 Wiley-VCH Verlag GmbH & Co. KGaA, Weinheim 

The time between successive frames was usually 100 or 130 ms—and sometimes up to 2 s—in order to record long-distance transport. The resolution was 146 nm per pixel for the Leica setup and 100 nm per pixel for the Zeiss setup.

### Scanning Fluorescence Correlation Spectroscopy (SFCS)

Vesicles containing 1 mol% of DSPE-PEG-biotin and no membrane labeling DiD were incubated with an excess amount of streptavidin/fluorescein-labeled streptavidin (500/1 molar ratio) to reach a fluorescent labeling density of 0.001 mol%. SFCS to determine the diffusion coefficient of the kinesin-1 lipid anchors was carried out on those vesicles (diameter $>20\,\mu m$) as described elsewhere in detail.[24]

### Vesicle Tracking

Vesicle tracking was carried out with the help of a Matlab routine in which the position of the vesicle was determined by its centre of mass. The image of the vesicle equator was convolved with a Gaussian kernel of $3\times3$ pixels and a variance of two, to reduce pixel noise effects. Afterwards, the threshold intensity was chosen with the aim to recover the bright rim of the equator of the vesicle as a closed circle in the binary image (with a pixel value of one in case the intensity is larger than the threshold intensity). Possible dark areas inside the vesicle rim were set to one, resulting in the vesicle appearing as a disc in the binary image whose centre of mass was calculated. Bright pixels outside the vesicle perimeter were discarded. The precision of this simple position determination was tested on non-moving adhered vesicles in the sample and found to be better than 30 nm if the vesicle radius was at least 1 μm.

The velocities of the transported vesicles were determined by cumulative summation of the distances travelled between at least ten consecutive frames (and only if the vesicle was transported along a single straight microtubule) and linear fitting of the resulting curve (Figure S3 of the Supporting Information). To avoid the influence of errors in the position determination perpendicular to the vesicle motion, all vesicle steps had been projected onto the contour of the microtubule filament before the cumulative sum was taken.

## Acknowledgements

*We thank Corina Bräuer for technical assistance and Martin Loose for purification of the kinesin. We acknowledge support from the Deutsche Forschungsgemeinschaft (Research Group FOR 877 and Heisenberg Programme), the Volkswagen Foundation (Grant I/84 087), the European Research Council (Starting Grant 242933), and the Max-Planck-Society.*

**Keywords:** biomimetics · cooperative transport · kinesin · nanotechnology · vesicles

[1] J. Howard, A. J. Hudspeth, R. D. Vale, *Nature* **1989**, *342*, 154 – 158.
[2] S. M. Block, L. S. Goldstein, B. J. Schnapp, *Nature* **1990**, *348*, 348 – 352.
[3] K. Svoboda, C. F. Schmidt, B. J. Schnapp, S. M. Block, *Nature* **1993**, *365*, 721 – 727.
[4] M. J. Schnitzer, K. Visscher, S. M. Block, *Nat. Cell Biol.* **2000**, *2*, 718 – 723.
[5] K. S. Thorn, J. A. Ubersax, R. D. Vale, *J. Cell Biol.* **2000**, *151*, 1093 – 1100.
[6] S. P. Gross, M. Vershinin, G. T. Shubeita, *Curr. Biol.* **2007**, *17*, R478-R486.
[7] J. Beeg, S. Klumpp, R. Dimova, R. S. Gracià, E. Unger, R. Lipowsky, *Biophys. J.* **2008**, *94*, 532 – 541.
[8] S. Klumpp, R. Lipowsky, *Proc. Natl. Acad. Sci. USA* **2005**, *102*, 17284 – 17289.
[9] K. Böhm, R. Stracke, P. Mühlig, E. Unger, *Nanotechnology* **2001**, *12*, 238 – 244.
[10] K. Visscher, M. J. Schnitzer, S. M. Block, *Nature* **1999**, *400*, 184 – 189.
[11] G. Koster, M. VanDuijn, B. Hofs, M. Dogterom, *Proc. Natl. Acad. Sci. USA* **2003**, *100*, 15583 – 15588.
[12] C. Leduc, O. Campàs, K. B. Zeldovich, A. Roux, P. Jolimaitre, L. Bourel-Bonnet, B. Goud, J.-F. Joanny, P. Bassereau, J. Prost, *Proc. Natl. Acad. Sci. USA* **2004**, *101*, 17096 – 17101.
[13] J. W. Murray, E. Bananis, A. W. Wolkoff, *Mol. Biol. Cell* **2000**, *11*, 419 – 433.
[14] E. Bananis, J. W. Murray, R. J. Stockert, P. Satir, A. W. Wolkoff, *J. Cell Biol.* **2000**, *151*, 179 – 186.
[15] C. Bottier, J. Fattaccioli, M. C. Tarhan, R. Yokokawa, F. O. Morin, B. Kim, D. Collard, H. Fujita, *Lab Chip* **2009**, *9*, 1694.
[16] H. W. Schroeder III, C. Mitchell, H. Shuman, E. L. F. Holzbaur, Y. E. Goldman, *Curr. Biol.* **2010**, *20*, 687 – 696.
[17] J. F. Nagle, S. Tristram-Nagle, *Biochim. Biophys. Acta* **2000**, *1469*, 159 – 195.
[18] C. Leduc, N. Pavin, F. Jülicher, S. Diez, *Phys. Rev. Lett.* **2010**, *105*, 128103.
[19] R. K. Doot, H. Hess, V. Vogel, *Soft Matter* **2007**, *3*, 349 – 356.
[20] K. R. Rogers, S. Weiss, I. Crevel, P. J. Brophy, M. Geeves, R. Cross, *EMBO J.* **2001**, *20*, 5101 – 5113.
[21] M. I. Angelova, S. Soléau, P. Méléard, J.-F. Faucon, P. Bothorel, *Prog. Colloid Polym. Sci.* **1992**, *89*, 127.
[22] B. Nitzsche, V. Bormuth, C. Bräuer, J. Howard, L. Ionov, J. Kerssemakers, T. Korten, C. Leduc, F. Ruhnow, S. Diez in *Methods in Cell Biology, Vol. 95* (Eds.: L. Wilson, J. J. Correia), Elsevier, **2010**, pp. 247 – 271.
[23] J. Helenius, G. Brouhard, Y. Kalaidzidis, S. Diez, J. Howard, *Nature* **2006**, *441*, 115 – 119.
[24] J. Ries, P. Schwille, *Biophys. J.* **2006**, *91*, 1915 – 1924.

Received: August 31, 2011
Revised: November 15, 2011
Published online on December 23, 2011

 © 2012 Wiley-VCH Verlag GmbH & Co. KGaA, Weinheim 